Article

pubs.acs.org/Biomac

Thermogelling Polymer–Platinum(IV) Conjugates for Long-Term Delivery of Cisplatin

Wenjia Shen,[†] Jiabin Luan,[†] Luping Cao,[†] Jian Sun,[†,‡] Lin Yu,*[,†] and Jiandong Ding[†]

[†]State Key Laboratory of Molecular Engineering of Polymers, Department of Macromolecular Science, Fudan University, Shanghai 200433, China

[‡]Department of Breast Surgery, Gynaecology and Obstetrics Hospital, Fudan University, Shanghai 200011, China

Supporting Information

ABSTRACT: In this study, we suggest a novel strategy of constituting an in situ-formed hydrogel composed of polymer–platinum(IV) conjugate to realize a long-term delivery of cisplatin. A unique conjugate was designed and synthesized by covalent linking of Pt(IV) complex to the hydrophobic end of two methoxyl poly(ethylene glycol)-*b*-poly(D,L-lactide) (mPEG–PLA) copolymer chains, resulting in the formation of Bi(mPEG–PLA)–Pt(IV). The conjugate could self-assemble into micelles in water, and its concentrated solution exhibited a thermoreversible sol–gel transition and formed a semisolid thermogel at body temperature. The incorporation of the cisplatin analogue Pt(IV) prodrug into the conjugate had a significant influence on its thermogelling properties and the conjugate thermogelation was attributed to the micellar aggregation. In vitro release experiments of Pt(IV)-conjugated thermogel showed that the platinum release lasted as long as two months. Furthermore, we demonstrated that the Pt(IV) prodrug was released mainly in the form of micelles and micellar aggregates from the gel depot. Compared with free cisplatin, the formation of conjugate micelles led to the enhanced in vitro cytotoxicity against cancer cells due to the effective accumulation into cells via endocytosis.

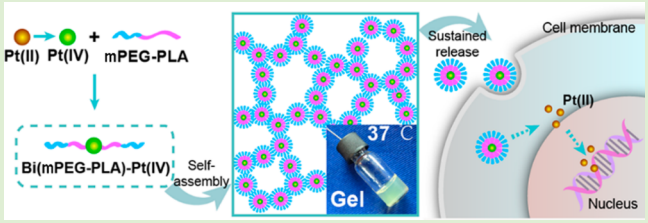

INTRODUCTION

Chemotherapy agents often cause severe toxicity. One of approaches to improve both the safety and efficacy of anticancer drugs is by local delivery,[1−5] which can maintain the drugs within the target tumor tissues at therapeutic concentrations for a long time due to the sustained drug release. Thermogelling polymers have been used to localize drug delivery for a long period.[2,6−13] Generally, these materials exhibited injectable sol states at low or room temperature and could spontaneously transform into gel states at the injection sites due to heating.[2,14−16] Typically biodegradable thermogels were composed of PEG/polyester block copolymers,[17−21] PEG/polypeptide block copolymers,[15,22] and poly(phosphazenes).[23,24] These amphiphilic thermogelling polymers self-assemble into micelles in water, and further, micellar aggregation upon heating leads to thermogelation.[2,19,25] Consequently, the thermogels are very suitable as carriers for hydrophobic anticancer drugs in a sustained release manner.[2,23] In contrast, a sustained delivery of hydrophilic anticancer drugs is challenging due to their rapid diffusion from the thermogel matrix, resulting in a high initial burst and severe side effects.[3,8]

We planned to conjugate anticancer drugs into thermogelling copolymers to resolve above-mentioned problems. Anticancer drug conjugation to biodegradable polymers has gained increased attention in the past decade.[24,26−31] Some polymer–drug conjugates have progressed to clinical studies.[26,28] These conjugates have demonstrated many advantages such as improving pharmacokinetics, enhancing antitumor activity and overcoming multidrug resistance (MDR).[29] The present work focused on designing and synthesizing polymer-cisplatin prodrug conjugates as a thermogelling system.

Cisplatin(II), a famous water-soluble anticancer drug, has been utilized to treat a variety of solid tumors such as testicular cancer, ovarian cancer, bronchogenic carcinoma, breast cancer, and so on.[32] It can preferentially bind with nucleophilic sites on guanine existing in DNA double-helix strands, thereby inhibiting replication and transcription of DNA, and ultimately resulting in cellular apoptosis.[32,33] However, cisplatin is readily attacked by protein in plasma,[34] leading to dramatical decrement of its therapeutic efficacy as well as causing severe side effects including nephrotoxicity, ototoxicity, neuropathy, nausea and vomiting, and drug resistance.[35,36] To date, great efforts have been made to develop new cisplatin analogues aimed at solving these problems.[32,37,38]

Among the numerous explored platinum compounds, octahedral complexes with Pt(IV) center are considered as potential prodrugs of Pt(II) due to the ability to overcome a number of shortcomings associated with cisplatin and its analogues.[32,39,40] These Pt(IV) compounds with octahedral structure are kinetically inert and thus exhibit less potency and

Received: August 19, 2014
Revised: October 23, 2014
Published: November 11, 2014

dx.doi.org/10.1021/bm501220a | *Biomacromolecules* 2015, 16, 105−115

toxicity than Pt(II).[39] However, they can be reduced to Pt(II) counterparts by glutathione, ascorbic acid or other reducing agents presenting in cancerous cells to regain their anticancer activity.[37] Moreover, two extra coordination sites on the octahedral Pt(IV) center provide more feasibility for further chemical modification.

Like other small molecular drugs, Pt(IV) compounds have some disadvantages such as rapid clearance from blood circulation and poor distribution to target sites. An effective strategy to overcome these problems is to load drugs into polymeric nanocarriers.[41−47] For example, Dhar et al. physically encapsulated a Pt(IV) prodrug into aptamer functionalized PEG−PLGA nanoparticles and confirmed an enhanced therapeutic efficacy against prostate cancer.[44] Recently, researchers have also combined the Pt(IV) complexes with polymer via covalent bonds (e.g., pH or reduction sensitive bond).[27,48−52] A polymer−Pt(IV) conjugate was prepared by Aryal et al. as an acid-responsive drug delivery system. The Pt(IV) complex was linked with a biocompatible diblock copolymer via a hydrazone bond and the corresponding nanoparticles exhibited a good acid-responsive drug release.[48] Also, Jing and co-workers synthesized methoxyl poly(ethylene glycol)-*b*-poly(ε-caprolactone)-*b*-poly(L-lysine) (mPEG-*b*-PCL-*b*-PLL) copolymer with free NH_2 side groups and conjugated Pt(IV) complexes to its side chains by amido bonds. The conjugates could self-assemble into micelles, and showed reduced systemic toxicity and enhanced anticancer activity.[27,53]

To the best of our knowledge, no thermogelling polymer−cisplatin prodrug conjugates have ever been reported. Meanwhile, none of cisplatin delivery systems has achieved a sustained release period as long as months. In the present work, we synthesized a unique conjugate and provided a proof-of-concept strategy to realize a long-term delivery of cisplatin over a period of months for the first time. The basic idea is schematically illustrated in Figure 1. We designed to bind a biocompatible and biodegradable diblock copolymer methoxyl poly(ethylene glycol)-*b*-poly(D,L-lactide) (mPEG−PLA) and a succinic acid modified Pt(IV) prodrug, which can be converted to cisplatin upon intracellular reduction.[49−51] The Pt(IV) prodrug was covalently conjugated to the PLA end of diblock copolymer with a stoichiometric ratio of 1/2, leading to a polymer−cisplatin prodrug conjugate, Bi(mPEG−PLA)−Pt(IV). Different from conventional approaches, in which the drug molecules were introduced into the conjugate by the modification of polymeric side chains or end groups,[24,31] our pathway affords the polymer−drug conjugate with explicit molecular structure and stable drug loading. We found that the conjugates could self-assemble into micelles in water and the concentrated aqueous polymer solution underwent a reversible sol−gel transition with increasing of temperature. Furthermore, we demonstrated that this polymer−cisplatin prodrug conjugate presented unique thermogelling properties, long-term drug release characteristics, and enhanced cytotoxicity against cancer cells.

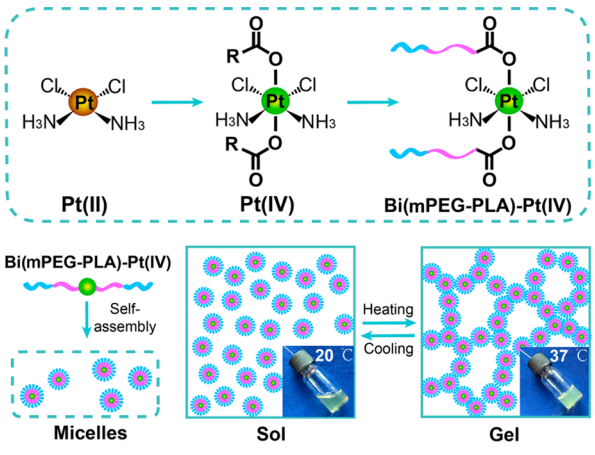

Figure 1. Molecular design of the unique polymer−Pt(IV) conjugate and corresponding thermogel. The resultant conjugates can self-assemble into micelles in water. The sol is a suspension of micelles at room temperature and spontaneously turns into a semisolid gel with percolated micelle network upon heating.

EXPERIMENTAL SECTION

Materials. Methoxyl poly(ethylene glycol) (mPEG) with molecular weight (MW) 750, stannous octoate ($Sn(Oct)_2$) of purity 95%, 4-dimethylaminopyridine (DMAP), and hexamethylene diisocyanate (HMDI) were products of Sigma-Aldrich. D,L-Lactide (LA) was purchased from Purac and used as received. Cisplatin of purity 99.6% was provided by Shandong Boyuan Pharmaceutical Co., Ltd. (China). Dicyclohexylcarbodiimide (DCC) was purchased from J&K Chemical. Other reagents were used without further purification.

Synthesis of mPEG−PLA Diblock Copolymers and mPEG−PLA−mPEG Triblock Copolymers. mPEG−PLA diblock copolymers were prepared via ring-opening polymerization in the presence of mPEG as the macroinitiator following the procedure described in our previous publications.[20,54] Briefly, 22.5 g (0.03 mol) mPEG 750 was put into a three-neck flask and heated under vacuum at 130 °C for 3 h to remove the residual moisture. Next, LA was added and heated under reduced pressure at 100 °C for 30 min. Then, 50 mg $Sn(Oct)_2$ was transferred into the mixtures, and the reaction system was heated with continuous stirring under an argon atmosphere at 150 °C for 12 h. Due to the insolubility of the required polymers in 80 °C water, crude products were purified by washing with 80 °C water four times to remove soluble and low MW byproducts. The residual water in the polymer was eliminated via freeze-drying and the final products were kept at −20 °C for further use.

Conventional mPEG−PLA−mPEG triblock copolymers were synthesized via coupling reaction in the presence of mPEG−PLA using HMDI as the coupling agent.[1,17] Briefly, mPEG−PLA (5 g, 0.002 mol) was dissolved in 50 mL of toluene, and the residual moisture in the polymer was removed by azeotropic distillation. Then, HMDI (0.17 g, 0.001 mol) and $Sn(Oct)_2$ (10 mg) were added into the reaction system and stirred at 60 °C for 6 h. After the solvent was distilled off to a final volume of 15 mL, the products were isolated by precipitation into ethyl ether and dried under vacuum.

Synthesis of Bi(mPEG−PLA)−Pt(IV) Conjugate. *a. Synthesis of cis,cis,trans-Diamminedichlorodihydroxy-platinum(IV) (cis,cis,-trans-Pt(NH$_3$)$_2$Cl$_2$(OH)$_2$) and cis,cis,trans-diamminedichlorodisuccinato-platinum (IV) (cis,cis,trans-Pt(NH$_3$)$_2$Cl$_2$(OOCCH$_2$CH$_2$COOH)$_2$).* *cis,cis,trans*-$Pt(NH_3)_2Cl_2(OH)_2$ and *cis,cis,trans*-$Pt(NH_3)_2Cl_2(OOCCH_2CH_2COOH)_2$ were synthesized according to the previously reported protocols.[49,51] Briefly, cisplatin was oxidized with 30% H_2O_2 in the dark at 70 °C for 2 h. The resultant product was isolated and purified. Then, *cis,cis,trans*-$Pt(NH_3)_2Cl_2(OH)_2$ (2.54 g), succinic anhydride (3.04 g), and anhydrated dimethyl sulfoxide (DMSO, 10 mL) were added into a 50 mL round-bottom flask and stirred in the dark under an argon atmosphere at 70 °C for 24 h. After removing the solvent through freeze-drying, the obtained solid was recrystallized from acetone and the pale yellow *cis,cis,trans*-$Pt(NH_3)_2Cl_2(OOCCH_2CH_2COOH)_2$ was collected.

b. Synthesis of Bi(mPEG−PLA)−Pt(IV) Conjugate. Diblock copolymer mPEG−PLA (4.0 g, 0.0015 mol) was dissolved in toluene and the residual moisture was removed by azeotropic distillation. Then, anhydrous dimethylformamide (DMF, 10 mL), *cis,cis,trans*-$Pt(NH_3)_2Cl_2(OOCCH_2CH_2COOH)_2$ (0.43 g, 0.0008 mol), DMAP

(0.38 g, 0.003 mol), and DCC (0.64 g, 0.003 mol) were added into the reaction system and kept stirring in the dark under an argon atmosphere for 36 h. The reaction mixture was then filtered and the crude conjugate was precipitated under −20 °C by slowly adding ethyl ether into the filtrate. The obtained yellow product was dialyzed against water for 12 h and lyophilized.

Physical−Chemical Characterization. ^{1}H NMR spectra were recorded on a 500 MHz proton NMR spectrometer (Bruker DMX 500) using tetramethylsilane as the internal standard. DMSO-d_6 and $CDCl_3$ were used as NMR solvents. MWs and their distributions of the copolymers were analyzed by a gel permeation chromatography (GPC) system (Agilent 1260) using DMF as solvent at the flow rate of 1.0 mL/min at 50 °C. Monodispersed poly(methyl methacrylate)s were used as the calibration standards. The conjugation yield was determined by coupled plasma optical emission spectrometer (ICP-OES, Hitachi P-4010). Intensity of spectral line at 265.945 nm was measured for all samples and standards. The platinum content in the samples was calculated via the standard curve of platinum.

Sol−Gel Transition. The sol−gel transition was determined via the test tube inverting method.[19,55] Polymer aqueous solutions with given concentrations were prepared in 2 mL vials. After equilibration at 4 °C overnight, the vials containing samples were immersed in a water bath at a designed temperature for 10 min and then inverted 180°. The sample was regarded as a gel if no visual flow was observed within 30 s. The temperature was increased 1 °C per step from 20 to 70 °C.

A dynamic stress-controlled rheometer (MCR 301, Anton Paar) was also used to investigate the thermo-induced sol−gel transitions of the polymer aqueous solutions. The measurements were operated with a cone plate (diameter: 60 mm, cone angle: 1°) at a fixed strain of 10% and an oscillation frequency of 10 rad/s. Temperature was controlled via a Peltier temperature controller with the increasing rate of 0.5 °C/min from 20 to 45 °C. A few drops of silicone oil were added onto the fringe of the cone to reduce the evaporation of solvent.

Determination of Critical Micellization Concentration (CMC). The CMC values were determined via the dye solubilization method using 1,6-diphenyl-1,3,5-hexatriene (DPH) as a hydrophobic dye.[56] A total of 50 μL of DPH stock solution (0.4 mM in methanol) was injected into 5 mL of polymer aqueous solutions at various concentrations ranging from 0.002 to 0.1 wt % and then stored overnight at 4 °C. After equilibration at 20 °C for 4 h, UV−vis spectra were recorded by a UV−vis spectrophotometer (Lambda 35) in the range of 320−420 nm. The CMC value was determined by plotting the difference in absorbance at 377 and 400 nm ($A_{377} - A_{400}$) versus logarithmic concentration.

Dynamic Light Scattering (DLS). DLS measurements were performed with a nanoparticle analyzer Zetasizer (Zetasizer Nano S90, Malvern) to investigate the micelle sizes and their distributions of polymer aqueous solutions as a function of concentration or temperature. Samples were treated by a 0.45 μm filter to remove possible dust before measurements and the light scattering angle was set as 90°. The hydrodynamic radius of particles was calculated according to the Stokes−Einstein equation.

Transmission Electron Microscopy (TEM). The Bi(mPEG−PLA)−Pt(IV) conjugate solution (20 μL, 1 wt %) was placed on a copper grid coated with a superthin carbon film and dried under an infrared lamp. The microscopic images were obtained by field emission transmission electron microscopy (FE-TEM, JEOL, JEM2100F) with an accelerating voltage of 200 kV.

In Vitro Drug Release. The Bi(mPEG−PLA)−Pt(IV) conjugate aqueous solution (25 wt %, 0.5 mL) was injected into a 15 mL vial (internal diameter: 22 mm) and equilibrated at 4 °C overnight. Next, the samples were incubated in a shaking bath (37 °C, 50 rpm) for 10 min to form stable thermogels. Then, 10 mL of PBS (pH 7.4) containing 0.025 wt % NaN_3 was added into the vials. At scheduled intervals, the release medium was taken out and replaced immediately with fresh PBS to keep the sink condition. The cisplatin-loaded mPEG−PLA thermogel (25 wt %) was set as the control and the platinum content of cisplatin was equal to that of the Bi(mPEG−PLA)−Pt(IV) thermogel. The platinum content in the release medium was determined by ICP-OES, and the cumulative release curve was calculated accordingly.

The release data were assessed via the classical models. The diffusion-controlled drug release from a polymeric system can be described via Higuchi equation[57] as written by

$$Q_t/Q = kt^{1/2}$$

Here, Q_t means the cumulative release at the time of t, and Q is the final release amount at infinite time. The coefficient k is a constant related to diffusivity, hydrogel chemical structure, and some geometric parameters.

Moreover, DLS and TEM measurements of the release medium at predetermined time intervals were performed to investigate the possible release mechanism. To ensure high polymer concentration in the released medium, the sampling interval was set as 5 days.

Cellular Experiments. *a. Cell Culture.* The human breast cancer cell line MDA-MB-231 was obtained from the Cell Bank of the Chinese Academy of Sciences (Shanghai, China). The cells were maintained in L15 medium (Gibco) containing 10% fetal bovine serum, 100 U/mL penicillin, and 100 mg/mL streptomycin under a humidified atmosphere containing 5% CO_2 at 37 °C.

b. In Vitro Cytotoxicity. LIVE/DEAD viability/cytotoxicity assay was performed to evaluate the cytotoxicity of the polymers qualitatively. MDA-MB-231 cells were seeded in 12-well tissue culture plates (5×10^4 cell/well) and incubated for 12 h. Then, the cells were treated with fresh medium (1 mL per well) containing free cisplatin, mPEG−PLA polymer or Bi(mPEG−PLA)−Pt(IV) conjugate (molar concentration equivalent to 100 μg/mL cisplatin) for 48 h. Afterward, cells were stained via ethidium homodimer-1 (2 μM in PBS) and calcein AM (1 μM in PBS) for 30 min following the protocol provided by the manufacturer and then observed by an inverted fluorescence microscopy (Axiovert 200, Zeiss).

Cytotoxicity of Bi(mPEG−PLA)−Pt(IV) conjugate was further quantitatively determined by the Cell Counting Kit-8 (CCK-8) assays. MDA-MB-231 cells were seeded in 96-well plates (2×10^4 cell/well) and incubated for 12 h. Then, the medium was replaced with 200 μL of fresh culture medium containing free cisplatin, mPEG−PLA polymer, and Bi(mPEG−PLA)−Pt(IV) conjugate at various concentrations, and the cells were postincubated for 48 h. Subsequently, the medium was removed and 200 μL of fresh medium containing 20 μL of CCK-8 solution was added into each well and another incubation of 3 h was required. Finally, the absorbance at 450 nm in each well was determined using a microplate reader (Multiskan Mk 3). The relative cell viability was calculated to quantify the cytotoxicity; the control group without treatment of any material in culture medium was defined as 100% viability; mPEG−PLA and free cisplatin at various concentrations were set as negative and positive controls, respectively.

c. In Vitro Cellular Uptake Studies. The cellular uptake of Bi(mPEG−PLA)−Pt(IV) conjugate micelles was investigated in the presence of coumarin-6 (Co-6) as a fluorescence probe. Two methods were used to prepare Co-6-loaded Bi(mPEG−PLA)−Pt(IV) conjugate micelles. In Method A, excess Co-6 was directly added into the Bi(mPEG−PLA)−Pt(IV) conjugate solution and stirred until saturation. The insoluble Co-6 powder was removed by filtration and the corresponding solution was prepared. In Method B, Co-6 (20 mg) and a certain amount of Bi(mPEG−PLA)−Pt(IV) conjugate were dissolved in 4 mL of CH_2Cl_2 and then the solvent was removed by rotary evaporation. Finally, the mixture was dissolved in L15 medium and a homogeneously yellow green solution was obtained after filtration using a 0.45 μm filter. The amount of Co-6 loaded in micelle solutions based on Methods A and B was determined by HPLC. MDA-MB-231 cells were seeded onto glass slides in 12-well plates (5×10^4 cell/well) and incubated for 24 h. Next, the medium was replaced with 1 mL of fresh medium containing Co-6-loaded Bi(mPEG−PLA)−Pt(IV) conjugate solutions based on Methods A and B (cisplatin concentration equal to 100 μg/mL in Bi(mPEG−PLA)−Pt(IV) conjugate solution) and saturated Co-6 solution (Free Co-6), respectively, and the cells were incubated for 4 h. Then, the cells were washed three times with PBS and fixed with 4 wt %

paraformaldehyde solution. A total of 15 min later, the fixative solution was removed and the cells were further rinsed three times with PBS. Finally, 0.4 mL of Triton X-100 solution (0.1 wt % in PBS) were added into each well for DAPI staining (5 min) and washed again with PBS. Cellular uptake of micelles was observed by Confocal Laser Scanning Microscope (CLSM, Leica SP5 II) under the FITC and DAPI channel, respectively.

RESULTS AND DISCUSSION

Synthesis and Characterization of Bi(mPEG−PLA)−Pt(IV) Conjugate. The Bi(mPEG−PLA)−Pt(IV) conjugate was synthesized according to the procedure, as illustrated in Scheme 1. Cisplatin was oxidized with H_2O_2 to *cis,cis,trans*-$Pt(NH_3)_2Cl_2(OOCCH_2CH_2COOH)_2$, mPEG−PLA, and Bi(mPEG−PLA)−Pt(IV), and all the characteristic proton signals were well assigned on the spectra. For *cis,cis,trans*-$Pt(NH_3)_2Cl_2(OOCCH_2CH_2COOH)_2$, the peaks at 12.07, 6.48, and 2.51 ppm were assigned to the proton signals of -COO***H***, -N***H***$_3$, and -C***H***$_2$CH$_2$COOH, respectively. Their corresponding molar ratio was approximately 1:3:2 according to the integral of the peak areas, indicating the successful synthesis of the dicarboxyl Pt(IV) complex with high purification. The number-average MW of mPEG−PLA was calculated via the peak areas at 3.38 ppm (-OC***H***$_3$) and 5.20 ppm (-C***H***(CH$_3$)COO-) based on the protocol described elsewhere.[58] Compared with mPEG−PLA, two new proton peaks at 5.97 and 2.66 ppm appeared in the ^{1}H NMR spectrum of Bi(mPEG−PLA)−Pt(IV) conjugate, as indexed in Figure 2c, which were assigned to the proton signals of -N***H***$_3$ and -OOCC***H***$_2$C***H***$_2$COO-, respectively. Importantly, the molar ratio among the peaks ***b*** (-N***H***$_3$), ***h*** (-OC***H***$_3$), and ***j*** (-OOCC***H***$_2$C***H***$_2$COO-) was approximately 3:3:4. This feature confirmed the successful coupling of mPEG−PLA into Bi(mPEG−PLA)−Pt(IV) conjugate in the presence of dicarboxyl Pt(IV) complex.

Scheme 1. Synthesis Procedure of Bi(mPEG−PLA)−Pt(IV) Conjugate

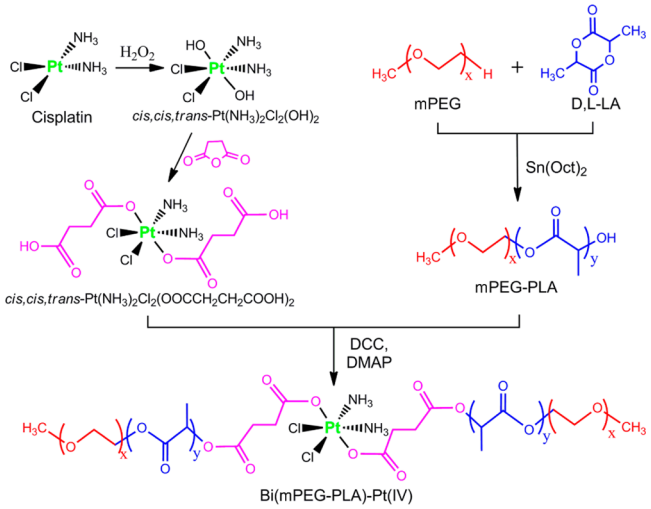

Table 1. Parameters of Polymers Synthesized in This Study

sample name	M_n[a]	M_n[b]	M_w/M_n[b]	sol−gel transition temperature[c] (°C)
mPEG−PLA	750−1895	2380	1.59	37
Bi(mPEG−PLA)−Pt(IV)	750−4030−750	4330	1.29	33
mPEG−PLA−mPEG	750−4060−750	4650	1.27	48

[a]M_n of mPEG block was provided by Aldrich and M_n of PLA blocks was calculated via ^{1}H NMR. [b]Measured by GPC. [c]Determined via test tube inverting method. Polymer concentration was 25 wt % in water.

$Pt(NH_3)_2Cl_2(OH)_2$, a Pt(IV) compound with two extra hydroxyl groups, and then reacted with succinic anhydride to produce *cis,cis,trans*-$Pt(NH_3)_2Cl_2(OOCCH_2CH_2COOH)_2$. mPEG−PLA diblock copolymer was prepared via ring-opening polymerization of LA using mPEG 750 as the macroinitiator and $Sn(Oct)_2$ as the catalyst. The Pt(IV) complex with two functional carboxyl groups was used as the coupling agent to link with mPEG−PLA, resulting in the formation of Bi(mPEG−PLA)−Pt(IV) conjugate. The resultant conjugates presented a pale yellow, sticky paste in bulk state. In addition, a conventional mPEG−PLA−mPEG triblock copolymer was synthesized in the presence of HMDI as the coupling agent.[1,17]

The entire reaction process of Bi(mPEG−PLA)−Pt(IV) conjugate was monitored via ^{1}H NMR measurements. Figure 2 shows the ^{1}H NMR spectra of *cis,cis,trans*-Pt-

Figure 3 shows the GPC chromatograms of mPEG-750, mPEG−PLA, mPEG−PLA−mPEG, and Bi(mPEG−PLA)−Pt(IV), respectively. The GPC traces of the Bi(mPEG−PLA)−Pt(IV) conjugate and mPEG−PLA−mPEG polymer displayed a unimodal manner with dispersity less than 1.3. Moreover, their MWs significantly increased and their dispersities correspondingly reduced compared with the mPEG−PLA polymer, indicating the successful formation of coupling products.[59] Table 1 summaries the parameters of polymers investigated in this study.

The formation of Bi(mPEG−PLA)−Pt(IV) conjugate was further confirmed by the analysis of platinum content using ICP-OES. The platinum content of Bi(mPEG−PLA)−Pt(IV) conjugate reached 3.36 wt %, which was very close to the theoretical calculation of 3.40 wt %. This finding provided a strong evidence of the high conjugation efficiency.

Sol−Gel Transition of Bi(mPEG−PLA)−Pt(IV) Conjugate in Water. Both mPEG−PLA polymer and Bi(mPEG−PLA)−Pt(IV) conjugate were soluble in water and formed low-viscous sols at low or ambient temperature. As the temperature increased, their aqueous solutions spontaneously turned into semisolid thermogels. Figure 4a presents the sol states of polymer/water system at room temperature (20 °C) and their corresponding gel states at body temperature (37 °C). Different from the colorless mPEG−PLA aqueous solution, the Bi(mPEG−PLA)−Pt(IV) conjugate in water exhibited a pale yellow state due to the introduction of pale yellow Pt(IV) complex into the polymer.

The phase diagrams of Bi(mPEG−PLA)−Pt(IV) conjugate, mPEG−PLA diblock copolymer, and mPEG−PLA−mPEG triblock copolymer are displayed in Figure 4b, which were determined via the test tube inverting method.[20] Some key parameters including sol−gel transition temperature, critical gelation concentration (CGC) and gel window width were obtained via phase diagram measurements. All the polymer/water systems underwent sol−gel−sol (suspension) transition upon heat stimulus. The sol (suspension) state represents that a gel originally becomes a flowable sol and subsequently the polymers precipitate in water. The sol−gel transition temperatures exhibited a weak concentration dependency, while the corresponding gel−sol (suspension) transition temperatures were more influenced by concentration.

dx.doi.org/10.1021/bm501220a | Biomacromolecules 2015, 16, 105−115

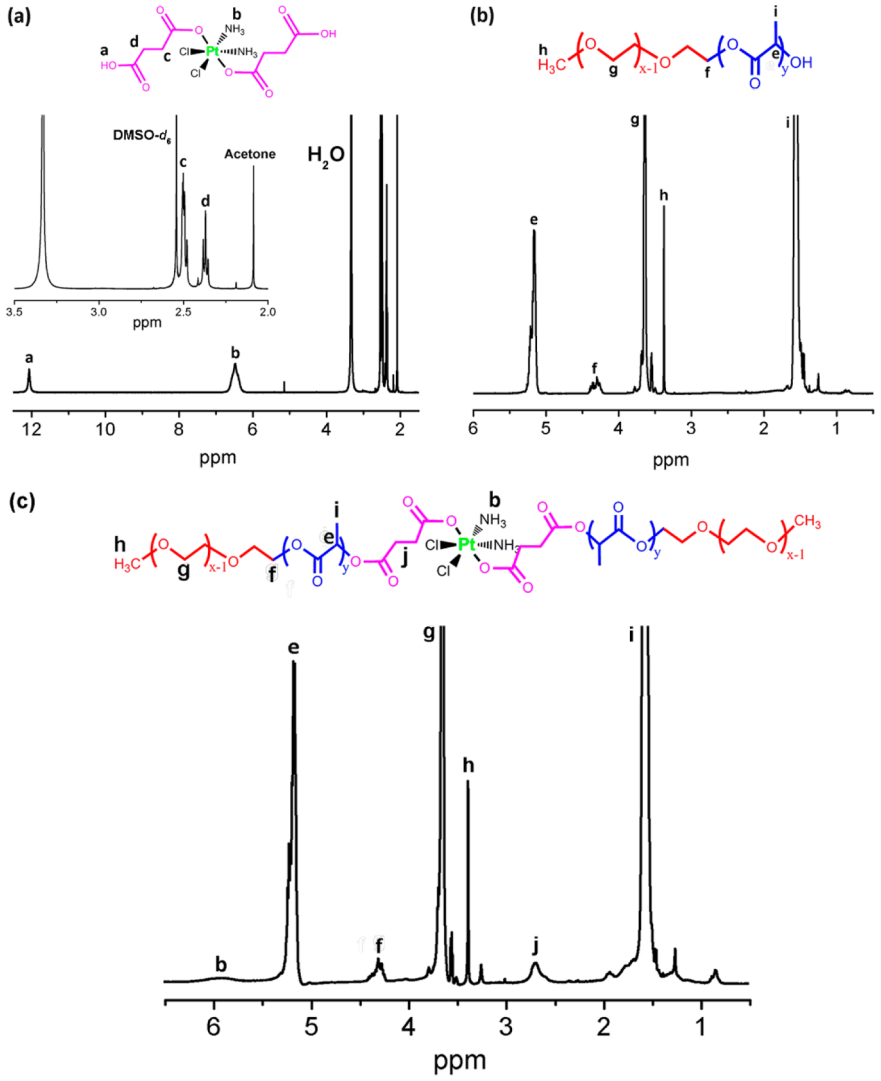

Figure 2. ^{1}H NMR spectra of the indicated samples (a) *cis,cis,trans*-Pt$(NH_3)_2Cl_2(OOCCH_2CH_2COOH)_2$ in DMSO-d_6, (b) mPEG–PLA, and (c) Bi(mPEG–PLA)–Pt(IV) in $CDCl_3$.

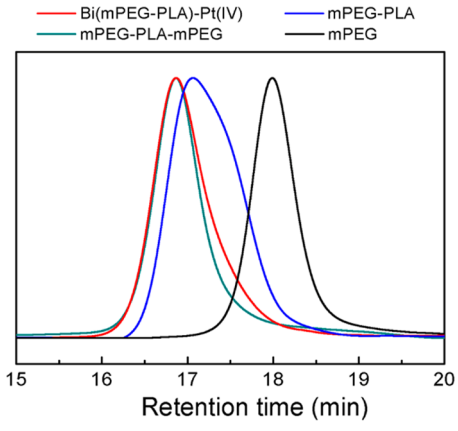

Figure 3. GPC chromatograms of the indicated polymers.

In general, the sol–gel transition temperature of conventionally thermogelling PEG–polyester–PEG triblock copolymers, which were prepared by coupling of PEG–polyester with HMDI, was remarkably higher than that of originally thermogelling PEG–polyester diblock copolymers.[58,60] In this study, a similar result was obtained. The sol–gel transition temperatures were elevated more than 10 °C and the CGC increased from 13 wt % to 16 wt % as the mPEG–PLA diblock copolymer converted to the mPEG–PLA–mPEG triblock copolymer. Consequently, the mPEG–PLA–mPEG/water system only presented a stable sol state at body temperature. Fortunately, the introduction of Pt(IV) complex into the Bi(mPEG–PLA)–Pt(IV) conjugate enhanced its global hydrophobicity significantly, resulting in lower sol–gel transition temperatures and a smaller CGC but a wider gel window compared with the mPEG–PLA polymer system. This finding clearly demonstrates that the different coupling agents had a significant effect on the thermogelling behaviors of resultant copolymers. Meanwhile, the gel window of Bi(mPEG–PLA)–Pt(IV) conjugate covered over body temperature, suggesting its potential as an injectable in situ-gelling biomaterial.

Dynamic rheological analysis was used to measure modulus (G') and viscosity (η). The temperature dependence of G' and η for Bi(mPEG–PLA)–Pt(IV) conjugate and mPEG–PLA polymer in water (25 wt %) is shown in Figure 5. Both polymer aqueous solutions were free-flowing sols with low modulus (less than 0.01 Pa) at low or room temperature, reflecting their good injectability. As the temperature increased, their solutions underwent an abrupt modulus change and the increase of G'

dx.doi.org/10.1021/bm501220a | *Biomacromolecules* 2015, 16, 105–115

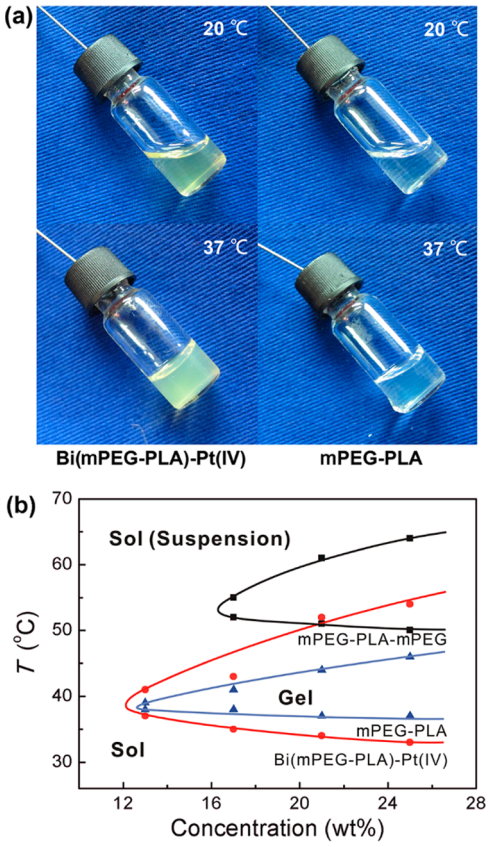

Figure 4. (a) Images of polymeric aqueous systems exhibiting sol states at 20 °C and gel states at 37 °C. Concentration: 25 wt %. (b) Phase diagrams of the indicated samples in water.

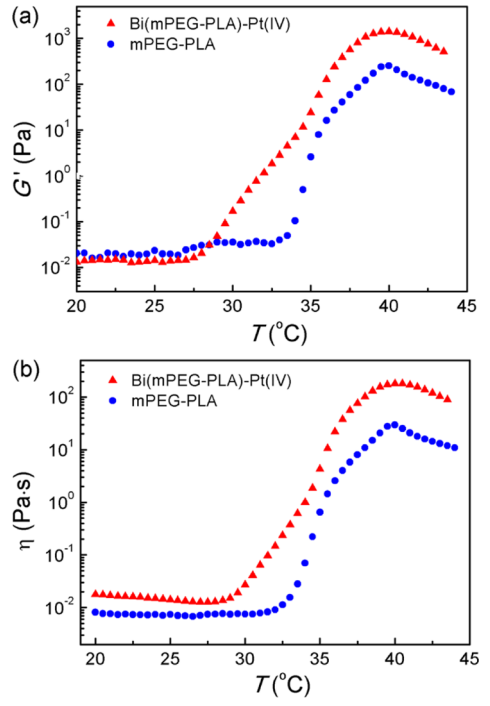

Figure 5. Storage modulus G' (a) and viscosity η (b) of the indicated polymers in water (25 wt %) as a function of temperature. Heating rates: 0.5 °C/min; oscillatory frequency: 10 rad/s.

spanned several orders of magnitude. Generally speaking, a dramatic increase of G' corresponds to a sol−gel transition. The transition temperatures of Bi(mPEG−PLA)−Pt(IV) and mPEG−PLA aqueous systems (25 wt %) obtained via the tube inverting approach were 33 and 37 °C, respectively (Figure 4b), which were consistent with the transition temperatures determined by rheological measurements. Meanwhile, compared with mPEG−PLA, the maximum modulus of polymer−Pt(IV) conjugate increased almost 1 order of magnitude to 10^3 Pa. The change of viscosity with temperature presented in a similar trend for these two polymer/water systems (Figure 5b).

Micelle Behaviors. Generally, amphiphilic PEG/polyester copolymers easily self-assemble into micelles in water.[20,25,61] Hydrophobic polyester segments constitute the micellar core while hydrophilic PEG chains occupy the micellar corona. The formation of core−corona structure could be confirmed via the hydrophobic dye method in the presence of polymer.[20,61] As shown in Figure 6a, the hydrophobic dye DPH entered the hydrophobic cores preferentially with the formation of micelles, resulting in the increase of absorbance at 337, 356, and 377 nm. The CMC values were determined by the absorbance difference between 377 and 400 nm as a function of concentration. Bi(mPEG−PLA)−Pt(IV) conjugate formed micelles with increasing of concentration and its CMC value was 0.0227 wt %. mPEG−PLA also formed micelles as a function of concentration and its CMC value was very close to that of Bi(mPEG−PLA)−Pt(IV) conjugate (see Supporting Information (SI), Figure S1). The CMC measurements provide clear evidence for the process of micellization.

DLS measurements were performed to determine the hydrodynamic diameter (D_h) of micelles in water and its variation trend with temperature and concentration. Figure 6b shows the change of the micelle size and size distribution of Bi(mPEG−PLA)−Pt(IV) conjugate as a function of concentration. At the low concentrations (0.1 and 1.0 wt %), the micelles only presented a single-peak profile. When the polymer concentration increased to 3.0 wt %, a multipeak pattern appeared. These peaks were assigned to the individual micelles and grouped micelles, respectively. Interestingly, the size of individual micelle gradually decreased with increasing polymer concentration from 0.1 wt % to 15.0 wt %.

Figure 6c shows the change of average size of micelles with temperature at different concentrations. Below 25 °C, the micelle size slightly reduced with increasing of polymer concentration. This feature was attributed to a repulsive reaction between micelles and a similar phenomenon was also observed in thermogelling mPEG−PLGA−mPEG copolymer system.[61] Meanwhile, as the concentration varied from 0.1 to 3.0 wt %, the average size of micelles almost maintained as a constant regardless of temperature. This is quite different from ABA or BAB-type PEG/polyester triblock copolymers reported elsewhere, in which the micelle size increases obviously with temperature at a low polymer concentration,[18,20,61] and the original mPEG−PLA polymer in this study. At the same low concentration (0.1 wt %), the average size of mPEG−PLA micelles increased significantly as the temperature elevated (see SI, Figure S2). This finding indicated that the aggregation ability of Bi(mPEG−PLA)−Pt(IV) conjugate micelles at the low concentrations is much weaker than those of PEG/polyester triblock copolymers and PEG−polyester diblock copolymers. At the higher polymer concentration (15 wt %, above the CGC), the average micelle size did not obviously change at low or room temperature. However, the average size

dx.doi.org/10.1021/bm501220a | Biomacromolecules 2015, 16, 105−115

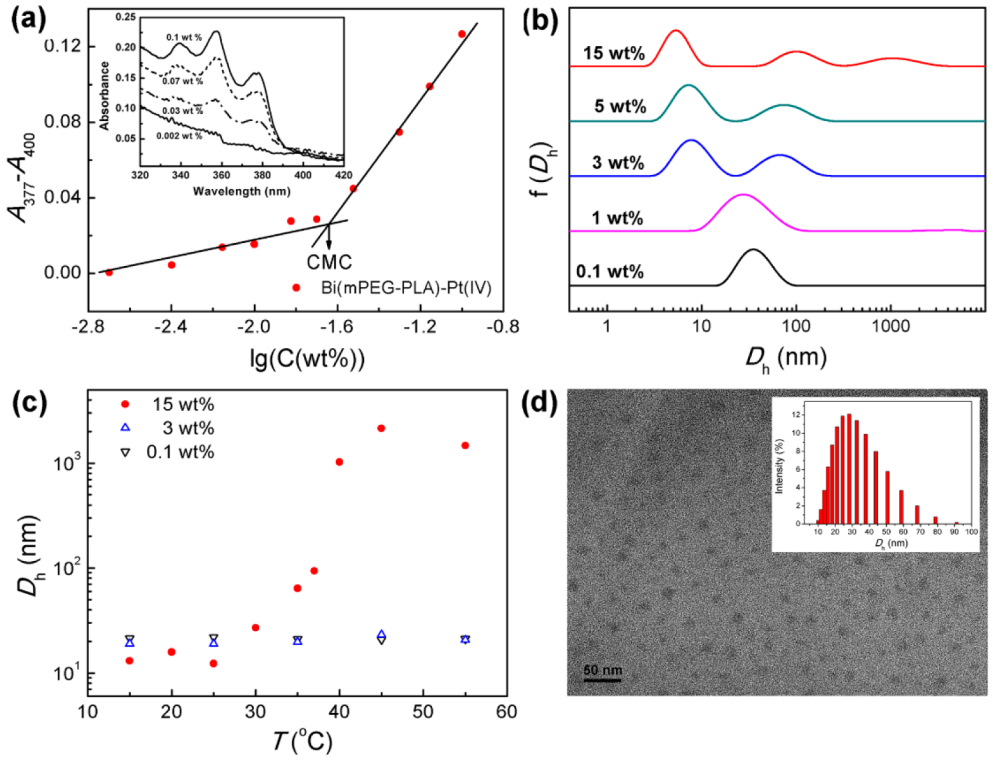

Figure 6. (a) CMC determination of Bi(mPEG−PLA)−Pt(IV) by extrapolation of the difference of absorbance at 377 and 400 nm. The measurements were carried out at 20 °C. UV−vis spectra of Bi(mPEG−PLA)−Pt(IV) aqueous solutions containing the hydrophobic dye (DPH) are inserted. DPH concentration was fixed at 4 μM as polymer concentration changed. For clarity, just four weight concentrations are presented. (b) Distribution of hydrodynamic diameter of micelles in Bi(mPEG−PLA)−Pt(IV) aqueous solutions at the indicated concentrations measured by DLS at 25 °C. (c) The average size variation of micelles as a function of temperature in Bi(mPEG−PLA)−Pt(IV) aqueous solutions at different polymer concentrations. (d) FE-TEM image showing the formation of micelles at a concentration of 1 wt % Bi(mPEG−PLA)−Pt(IV) conjugate in water.

increased abruptly near the sol−gel transition temperature. These results affirm that the micellar aggregation still occurred at its concentrated solution (above the CGC) with increasing of temperature although no sign of aggregation of micelles was observed at the lower concentrations. Consequently, the formation of a percolated micelle network via micellar aggregation, which have been used to illustrate the gelation mechanism for other PEG/polyester copolymers,[25,56] was responsible for the thermogelation of Bi(mPEG−PLA)−Pt(IV) conjugate in water.

Micelle formation was further supported by FE-TEM observation. A typical TEM image of micelles is visualized in Figure 6d. Since the observation was performed at the dry state, the size of micelles was smaller than that determined via DLS measurements at the sol state.

In Vitro Drug Release from Hydrogel. Drug release from the in situ-formed Bi(mPEG−PLA)−Pt(IV) thermogel was carried out under physiological conditions (pH 7.4 and 37 °C). The integrity of conjugate hydrogel was well-maintained in PBS over one and a half months (see SI, Figure S3). The platinum amount released was measured by ICP-OES. Figure 7 shows the cumulative release profile of platinum from the Bi(mPEG−PLA)−Pt(IV) thermogel. The platinum release lasted more than 60 days, and no significant initial burst was observed. It took 9 weeks to release 75% of the incorporated platinum. Considering that mPEG−PLA−mPEG aqueous system could not form a thermogel at 37 °C, mPEG−PLA was set as the control for directly physical encapsulation of free cisplatin. The result displays that free cisplatin completely released from the mPEG−PLA gel matrix within 12 h. Another PLA−PEG−PLA

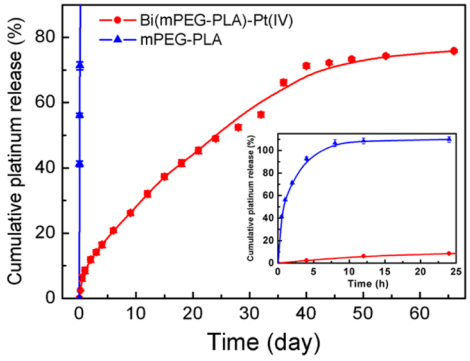

Figure 7. In vitro release profiles of platinum from Bi(mPEG−PLA)−Pt(IV) and mPEG−PLA thermogels. The Bi(mPEG−PLA)−Pt(IV) conjugate concentration is 25 wt % and the corresponding drug loading content for 25 wt % thermogel is 12.9 mg/mL of cisplatin. The mPEG−PLA thermogel contained the same cisplatin amount of Bi(mPEG−PLA)−Pt(IV) conjugate.

thermogel whose modulus was similar to the Bi(mPEG−PLA)−Pt(IV) thermogel was also used to encapsulate and release cisplatin. A similar result was achieved (see SI, Figure S4). Therefore, the sustained release of platinum from the thermogel depot was attributed to the conjugation of Pt(IV) complex into polymer via chemical bond and the formation of a stable thermogel. Moreover, it is worth pointing out that 3.36 wt % platinum content in the Bi(mPEG−PLA)−Pt(IV) conjugate is not very high compared with the other polymer systems.[27,51] However, as a polymer hydrogel, the Bi(mPEG−

dx.doi.org/10.1021/bm501220a | Biomacromolecules 2015, 16, 105−115

PLA)−Pt(IV) thermogel system can hold the high polymer concentration, and thus the shortcoming of low drug loading would be effectively offset. For example, the drug loading for 25 wt % thermogel reached 12.9 mg/mL of cisplatin. With increasing the polymer concentration to 30 wt % or above, the drug loading can further increase.

The released data were further fitted via Higuchi equation written as $Q_t/Q = kt^{1/2}$. The release profile was well consistent with the equation, and a good relevant coefficient R^2 (>0.99) was obtained, suggesting that the platinum released from the conjugate hydrogel was mainly governed by diffusion mechanism.

The released platinum detected via ICP-OES can provide the platinum amount precisely but not afford any information about its species during the release process. To obtain more information, the release media withdrawn at predetermined time points were measured by DLS and TEM, as shown in Figure 8. The results affirmed that the nanoparticles were

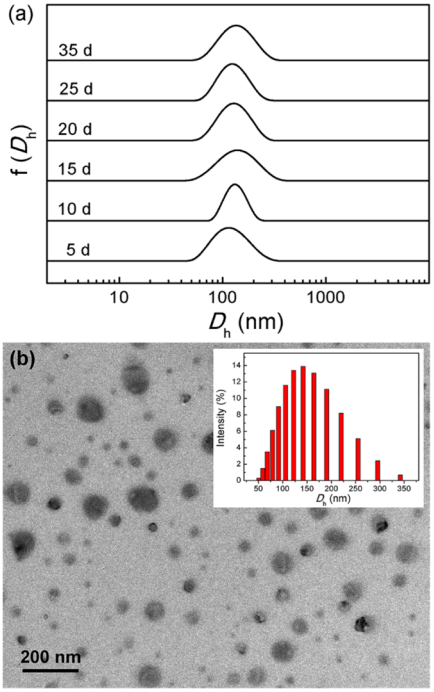

Figure 8. (a) Size distribution of nanoparticles at 25 °C in the release medium of Bi(mPEG−PLA)−Pt(IV) hydrogel at scheduled intervals; (b) TEM image of nanoparticles in the release medium at the 15th day.

released from the thermogel and the average diameter of particles was very stable during the whole release period. The micelles and their aggregates in similar size were detected in 15 wt % Bi(mPEG−PLA)−Pt(IV) conjugate aqueous solution as demonstrated in Figure 6b, suggesting that the Pt(IV) prodrug was mainly released in the form of micelles and micellar aggregates but not small molecules. The erosion of release medium was responsible for the breakup of micelles and their aggregates from the gel matrix. Such a result was consistent with the diffusion mechanism.

In Vitro Toxicity toward Tumor Cells of the Polymer−Pt(IV) Conjugate. To evaluate the efficacy of Bi(mPEG−PLA)-Pt(IV) conjugate as an anticancer prodrug, the in vitro cytotoxicity tests were first examined via LIVE/DEAD viability/cytotoxicity assay, in which the live and dead cells emitted green and red fluorescence, respectively. Human breast cancer cell line MDA-MB-231 was chosen as the model cancer cell due to the well-known anticancer efficacy of cisplatin against breast cancer.[62] Cells were cultured in L15 media containing free cisplatin or Bi(mPEG−PLA)−Pt(IV) conjugate with a fixed concentration (100 μg/mL cisplatin) for 48 h. The biocompatibility of mPEG−PLA polymer was also examined and its molar concentration was equal to that of Bi(mPEG−PLA)−Pt(IV) conjugate. As shown in Figure 9a, the negligible

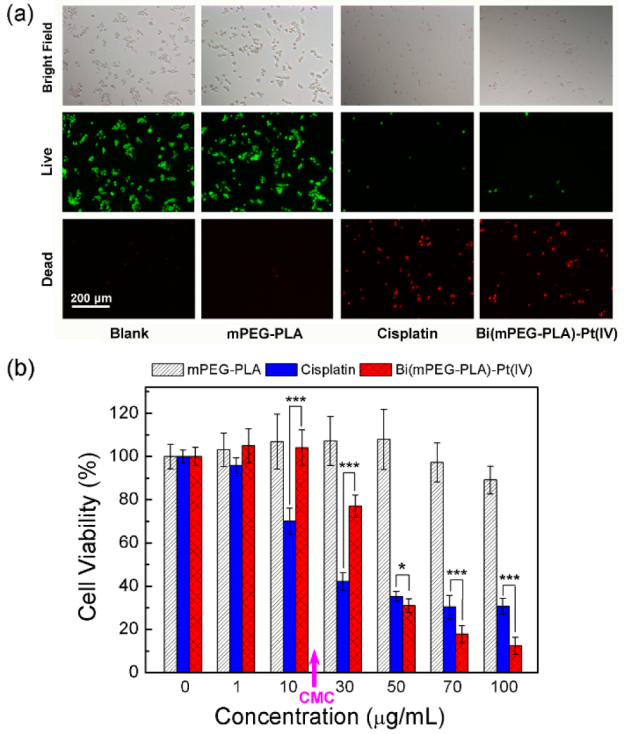

Figure 9. (a) Microscope images of MDA-MB-231 cells treated with indicated materials in medium to evaluate cytotoxicity. Line 1: Bright field microscope photographs; Line 2: corresponding fluorescence micrographs after LIVE/DEAD viability/cytotoxicity assay where live cells were stained by calcein AM (green); Line 3: corresponding fluorescence micrographs after live−dead straining where dead cells were stained by ethidium homodimer (red). Cells were cultured for 48 h and the same field of visions was used to take images per sample. (b) In vitro cytotoxicity of mPEG−PLA, free cisplatin, and Bi(mPEG−PLA)−Pt(IV) conjugate against MDA-MB-231 cells as a function of cisplatin concentration. The blank control with culture medium only was set as 100% cell viability. Each point represents the mean ± SD; $n = 6$. Significant differences between the groups of free cisplatin and Bi(mPEG-PLA)-Pt(IV) determined by Students' t-test are specially marked: $^*p < 0.05$; $^{***}p < 0.001$. The "CMC" represents the formation of Bi(mPEG−PLA)−Pt(IV) conjugate micelles and its corresponding cisplatin concentration was 11.73 μg/mL.

cytotoxicity of mPEG−PLA polymer against MDA-MB-231 cancer cells confirmed the good biocompatibility of the polymer itself. In contrast, most of the cells were dead after treating with cisplatin or Bi(mPEG−PLA)−Pt(IV) conjugate for 48 h. This result confirms the efficacy of Bi(mPEG−PLA)−Pt(IV) conjugate as an anticancer polymeric prodrug.

The cytotoxicity of Bi(mPEG−PLA)−Pt(IV) conjugate was further evaluated quantitatively via CCK-8 assay and the results are displayed in Figure 9b. MDA-MB-231 cancer cells were treated with free cisplatin and Bi(mPEG−PLA)−Pt(IV)

dx.doi.org/10.1021/bm501220a | Biomacromolecules 2015, 16, 105−115

aqueous solutions at various cisplatin concentrations ranging from 1 to 100 μg/mL. Consistent with the above results, very little cytotoxicity was detected for the mPEG−PLA itself. Even at the highest concentration of mPEG−PLA (2.4 mg/mL), the cell viability was still as high as 90%. Different from mPEG−PLA, both free cisplatin and Bi(mPEG−PLA)−Pt(IV) conjugate exhibited an increasing cytotoxicity with drug concentration. At the low drug concentrations, the cytotoxicity of free cisplatin was higher than that of Bi(mPEG−PLA)−Pt(IV) conjugate. However, the cytotoxicity of Bi(mPEG−PLA)−Pt(IV) conjugate exceeded that of free cisplatin at the high concentrations (50, 70, and 100 μg/mL). In particular, at the concentration of 100 μg/mL, its cell viability was only half of that of free cisplatin. The CMC value of Bi(mPEG−PLA)−Pt(IV) conjugate was 0.0227 wt % and its corresponding cisplatin concentration was 11.73 μg/mL. Combining with these results, we found that the cytotoxicity of Bi(mPEG−PLA)−Pt(IV) conjugate abruptly increased following the formation of micelles. Generally, a better accumulation into cells led to a higher cytotoxicity. Therefore, it is speculated that the cellular uptake of Bi(mPEG−PLA)−Pt(IV) conjugate was dramatically accelerated due to the formation of micelles, and subsequently the conjugated-Pt(IV) species was rapidly reduced to active Pt(II) species cisplatin to cross-link with DNA inside the cancer cells. This conclusion can be further supported by the cellular uptake experiments in the next section.

In Vitro Cellular Uptake. To visualize the cellular uptake of Bi(mPEG−PLA)−Pt(IV) conjugate micelles, Co-6, a hydrophobic probe, was used to label the micelles. Generally speaking, the hydrophobic substances could be physically encapsulated into the hydrophobic core of polymeric micelles. In the present study, we adopted two methods to enhance the solubility of Co-6 in the Bi(mPEG−PLA)−Pt(IV) conjugate micelles. We first tried to directly mix solid Co-6 with Bi(mPEG−PLA)−Pt(IV) conjugate solution (Method A). This method did not effectively increase the solubility of Co-6 and the loading amount of Co-6 in the Bi(mPEG−PLA)−Pt(IV) conjugate solution was just 0.35 μg/mL. Next, we tried another method, which consisted of two steps: (1) solvent evaporation and (2) dissolution together in water (Method B). This method increased the solubility of Co-6 to 10.75 μg/mL, and the resultant micelle solution exhibited a yellow green color. This result was attributed to the uniform distribution of Co-6 molecules into the polymeric conjugate after the solvent evaporation and then the effective solubilization along with the formation of micelles in water. Meanwhile, these Co-6 molecules loaded via Method B were stable and not easy to leak out from the micelles. This finding also suggests that the Bi(mPEG−PLA)−Pt(IV) conjugate itself can serve as a nanocarrier to deliver other hydrophobic drugs.

The cellular uptake of Co-6-labeled Bi(mPEG−PLA)−Pt(IV) conjugate micelles in MDA-MB-231 cells were observed by CLSM. Figure 10a presents the fluorescence micrographs of MDA-MB-231 cells 4 h after administration of the indicated samples. The nuclei of cells were stained with DAPI (blue). No green fluorescence was observed in the cells treated with L15 medium containing free Co-6. In the case of the cells treated with Co-6-labeled Bi(mPEG−PLA)−Pt(IV) conjugate micelles, which was obtained via Method A, only slight green fluorescence was observed due to the low amount of Co-6 in the micelles. In contrast, in the cells cultured with Co-6-labeled Bi(mPEG−PLA)−Pt(IV) conjugate micelles based on Method B, intense green fluorescence of Co-6 was observed. Overlay of the images taken from DAPI and Co-6 channels illustrated that the green fluorescence was full of the cytoplasm, suggesting that the polymer−drug conjugate micelles could efficiently enter the cancerous cells via endocytosis. Consequently, the endocytosis with high efficiency resulted in the enhanced cytotoxicity of Bi(mPEG−PLA)−Pt(IV) conjugate micelles as compared to that of free cisplatin, as demonstrated in Figure 9b. Furthermore, Figure 10b shows the fluorescence micrographs, in which the cells were treated with Co-6-labeled Bi(mPEG−PLA)−Pt(IV) conjugate micelles based on Method B, captured at three indicated incubation times. As the incubation time increased from 0.5 to 4 h, not only the fluorescence intensity of Co-6 in the cytoplasm increased obviously, but also the green fluorescence finally entered the cell nuclei.

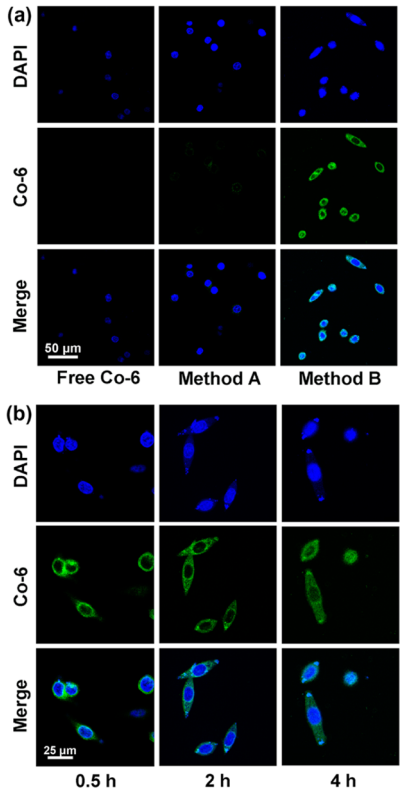

Figure 10. (a) Cellular uptake of Co-6-labeled Bi(mPEG−PLA)−Pt(IV) micelles in MDA-MB-231 cells after incubation for 4 h. CLSM images were taken from the DAPI channel (line 1, blue), the Co-6 channel (line 2, green), and merged images of the DAPI and Co-6 channels (line 3). Methods A and B represent two different methods that were used to prepare Co-6-labeled Bi(mPEG−PLA)−Pt(IV) conjugate micelles. (b) Cellular uptake of Co-6-labeled Bi(mPEG−PLA)−Pt(IV) conjugate micelles obtained via Method B after 0.5, 2, and 4 h of incubation.

At last, the injectable hydrogel formulations containing anticancer drugs were generally administrated via intratumoral injection.[3,23,24] Together with the in vitro anticancer efficacy of Bi(mPEG−PLA)−Pt(IV) conjugate micelles and the long-acting release profile of Bi(mPEG−PLA)−Pt(IV) conjugate thermogel, a potential application process of this polymer−Pt(IV) conjugate was proposed: after the intratumoral injection of Bi(mPEG−PLA)−Pt(IV) conjugate thermogel, polymer−Pt(IV) conjugate micelles gradually broke away from the hydrogel and entered the cells via endocytosis; then the micelles were broken into carrier polymers and cisplatin by

dx.doi.org/10.1021/bm501220a | Biomacromolecules 2015, 16, 105−115

intracellular reducing agents; and finally, cisplatin bound with DNA and exerted its efficacy. Such a reduction easily takes place due to the presence of sufficient reducing agents, such as mercaptan, glutathione, and others in the cancer cells.[49−51] This process is schematically presented in Figure 11.

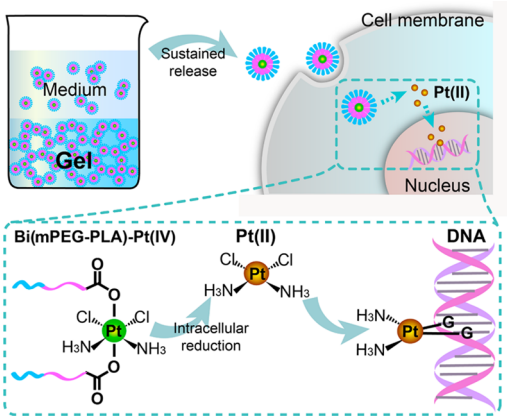

Figure 11. Schematic presentation of the injectable Bi(mPEG−PLA)−Pt(IV) conjugate thermogel as a localized and long-term cisplatin delivery system. The conjugate micelles and micellar aggregates would be released sustainably from the thermogel depot over a period of months. The corresponding micelles readily enter cancerous cells and then the active drug, cisplatin, is released upon intracellular reduction of polymer−Pt(IV) conjugates.

CONCLUSIONS

A novel prodrug conjugate Bi(mPEG−PLA)−Pt(IV) was designed and synthesized. Its uniqueness is that the hydrophobic segments of two mPEG−PLA polymer chains were linked to one Pt(IV) complex through covalent ester bonds. The introduction of cisplatin prodrug significantly enhanced the global hydrophobicity of Bi(mPEG−PLA)−Pt(IV) conjugate. As a result, the conjugate/water system exhibited a free-flowing sol with good injectability at low or room temperature and spontaneously turned into a semisolid gel at body temperature. Moreover, the amphiphilic conjugates could self-assemble into micelles in water and micelle aggregation was responsible for its in situ thermogelation.

A sustained platinum release from the conjugate thermogel without initial burst was achieved up to two months and thus the longest-acting delivery system of cisplatin was realized by us so far. Further experiments confirmed that the Pt(IV) prodrug was mainly released in the form of micelles and micelle aggregates, which broke away from the thermogel matrix. Also, the in vitro cytotoxicity of Bi(mPEG−PLA)−Pt(IV) conjugate was confirmed via CCK-8 assay on MDA-MB-231 cancer cells. Its enhanced cytotoxicity against tumor cells as compared to free cisplatin was attributed to the formation of micelles. The conjugate micelles could be effectively internalized by the cells through endocytosis and then the active Pt(II) species cisplatin was rapidly released due to the facilitated intracellular reduction.

These results suggest that the polymer−Pt(IV) conjugate thermogel as an injectable polymeric prodrug affords an efficient pathway to sustain delivery of cisplatin for a long period. Moreover, our current research also provides a potentially important platform technology for sustained delivery of other therapeutic or diagnostic agents based on covalently linking drug molecules onto thermogelling polymers through double or multiple functional linkers.

ASSOCIATED CONTENT

Supporting Information

The CMC values of both Bi(mPEG−PLA)−Pt(IV) conjugate and mPEG−PLA polymer, the distribution of hydrodynamic diameter of their corresponding micelles formed in water as a function of temperature, the photographs of both Bi(mPEG−PLA)−Pt(IV) conjugate and mPEG−PLA polymer hydrogels in PBS at 37 °C as a function of incubation time, and the in vitro release profile of platinum release from cisplatin-loaded PLA−PEG−PLA thermogel. This material is available free of charge via the Internet at http://pubs.acs.org.

AUTHOR INFORMATION

Corresponding Author

*Tel.: +86-21-65642531. Fax: +86-21-65640293. E-mail: yu_lin@fudan.edu.cn.

Notes

The authors declare no competing financial interest.

ACKNOWLEDGMENTS

The group was supported by NSF of China (Grant Nos. 51273217, 91127028, and 21034002), Chinese Ministry of Science and Technology (973 Program No. 2011CB606203), Science and Technology Developing Foundation of Shanghai (Grant Nos. 12JC1402600 and 14441901500), Project of Shanghai municipal Health Bureau (Grant No. 2010049), and Jiangsu Key Laboratory of Advanced Functional Polymer Design and Application (Soochow University).

REFERENCES

(1) Jeong, B.; Bae, Y. H.; Lee, D. S.; Kim, S. W. *Nature* **1997**, *388*, 860−862.
(2) Yu, L.; Ding, J. D. *Chem. Soc. Rev.* **2008**, *37*, 1473−1481.
(3) Chang, G. T.; Ci, T. Y.; Yu, L.; Ding, J. D. *J. Controlled Release* **2011**, *156*, 21−27.
(4) Vermonden, T.; Censi, R.; Hennink, W. E. *Chem. Rev.* **2012**, *112*, 2853−2888.
(5) Tsao, C. T.; Kievit, F. M.; Ravanpay, A.; Erickson, A. E.; Jensen, M. C.; Ellenbogen, R. G.; Zhang, M. *Biomacromolecules* **2014**, *15*, 2656−2662.
(6) Huynh, C. T.; Nguyen, M. K.; Lee, D. S. *Macromolecules* **2011**, *44*, 6629−6636.
(7) Li, K.; Yu, L.; Liu, X. J.; Chen, C.; Chen, Q. H.; Ding, J. D. *Biomaterials* **2013**, *34*, 2834−2842.
(8) Yu, L.; Ci, T. Y.; Zhou, S. C.; Zeng, W. J.; Ding, J. D. *Biomater. Sci.* **2013**, *1*, 411−420.
(9) Ci, T. Y.; Chen, L.; Yu, L.; Ding, J. D. *Sci. Rep.* **2014**, *4*, 5473.
(10) Fang, F.; Gong, C. Y.; Qian, Z. Y.; Zhang, X. N.; Gou, M. L.; You, C.; Zhou, L. X.; Liu, J. G.; Zhang, Y.; Guo, G.; Gu, Y. C.; Luo, F.; Chen, L. J.; Zhao, X.; Wei, Y. Q. *ACS Nano* **2009**, *3*, 4080−4088.
(11) Qian, Z. Y.; Fu, S. Z.; Feng, S. S. *Nanomedicine (London, U. K.)* **2013**, *8*, 161−164.
(12) Wang, C.; Long, C. F.; Xie, C. S.; Chen, X. X.; Zhang, L.; Chu, B. Y.; Wang, Y. J.; Luo, F.; Qian, Z. Y. *J. Biomed. Nanotechnol.* **2013**, *9*, 357−366.
(13) Song, F. F.; Li, X. Q.; Wang, Q.; Liao, L. Q.; Zhang, C. *J. Biomed. Nanotechnol.* **2015**, *11*, 40−52.
(14) Liu, C. D.; Zhang, Z.; Liu, K. L.; Ni, X.; Li, J. *Soft Matter* **2013**, *9*, 787−794.
(15) Park, M. H.; Joo, M. K.; Choi, B. G.; Jeong, B. *Acc. Chem. Res.* **2012**, *45*, 424−433.

(16) Zhang, Z. X.; Liu, K. L.; Li, J. *Angew. Chem., Int. Ed.* **2013**, *52*, 6180−6184.
(17) Jeong, B.; Bae, Y. H.; Kim, S. W. *Macromolecules* **1999**, *32*, 7064−7069.
(18) Shim, M. S.; Lee, H. T.; Shim, W. S.; Park, I.; Lee, H.; Chang, T.; Kim, S. W.; Lee, D. S. *J. Biomed. Mater. Res.* **2002**, *61*, 188−196.
(19) Yu, L.; Zhang, H.; Ding, J. D. *Angew. Chem., Int. Ed.* **2006**, *45*, 2232−2235.
(20) Yu, L.; Zhang, Z.; Ding, J. D. *Biomacromolecules* **2011**, *12*, 1290−1297.
(21) Petit, A.; Müller, B.; Meijboom, R.; Bruin, P.; van de Manakker, F.; Versluijs-Helder, M.; de Leede, L. G. J.; Doornbos, A.; Landin, M.; Hennink, W. E.; Vermonden, T. *Biomacromolecules* **2013**, *14*, 3172−3182.
(22) Yeon, B.; Park, M. H.; Moon, H. J.; Kim, S. J.; Cheon, Y. W.; Jeong, B. *Biomacromolecules* **2013**, *14*, 3256−3266.
(23) Cho, J. K.; Hong, J. M.; Han, T.; Yang, H. K.; Song, S. C. *J. Drug Target.* **2013**, *21*, 564−573.
(24) Chun, C.; Lee, S. M.; Kim, S. Y.; Yang, H. K.; Song, S. C. *Biomaterials* **2009**, *30*, 2349−2360.
(25) Yu, L.; Chang, G. T.; Zhang, H.; Ding, J. D. *J. Polym. Sci., Part A: Polym. Chem.* **2007**, *45*, 1122−1133.
(26) Vasey, P. A.; Kaye, S. B.; Morrison, R. *Clin. Cancer Res.* **1999**, *5*, 83−94.
(27) Xiao, H. H.; Qi, R. G.; Liu, S.; Hu, X. L.; Duan, T. C.; Zheng, Y. H.; Huang, Y. B.; Jing, X. B. *Biomaterials* **2011**, *32*, 7732−7739.
(28) Duncan, R.; Vicent, M. J. *Adv. Drug Delivery Rev.* **2013**, *65*, 60−70.
(29) Delplace, V.; Couvreur, P.; Nicolas, J. *Polym. Chem.* **2014**, *5*, 1529−1544.
(30) Zhang, S.; Zou, J.; Elsabahy, M.; Karwa, A.; Li, A.; Moore, D. A.; Dorshow, R. B.; Wooley, K. L. *Chem. Sci.* **2013**, *4*, 2122−2126.
(31) Lin, X. N.; Deng, L. D.; Xu, Y. S.; Dong, A. J. *Soft Matter* **2012**, *8*, 3470−3477.
(32) Kelland, L. *Nat. Rev. Cancer* **2007**, *7*, 573−584.
(33) Jung, Y.; Lippard, S. J. *Chem. Rev.* **2006**, *107*, 1387−1407.
(34) Ivanov, A. I.; Christodoulou, J.; Parkinson, J. A.; Barnham, K. J.; Tucker, A.; Woodrow, J.; Sadler, P. J. *J. Biol. Chem.* **1998**, *273*, 14721−14730.
(35) Deconti, R. C.; Toftness, B. R.; Lange, R. C. *Cancer Res.* **1973**, *33*, 1310−1315.
(36) Rabik, C. A.; Dolan, M. E. *Cancer Treat. Rev.* **2007**, *33*, 9−23.
(37) Wong, E.; Giandomenico, C. M. *Chem. Rev.* **1999**, *99*, 2451−2466.
(38) Bruijnincx, P. C.; Sadler, P. J. *Curr. Opin. Chem. Biol.* **2008**, *12*, 197−206.
(39) Hall, M. D.; Mellor, H. R.; Callaghan, R.; Hambley, T. W. *J. Med. Chem.* **2007**, *50*, 3403−3411.
(40) Reithofer, M.; Galanski, M.; Roller, A.; Keppler, B. K. *Eur. J. Inorg. Chem.* **2006**, 2612−2617.
(41) Wang, H.; Tang, L.; Tu, C. L.; Song, Z. Y.; Yin, Q.; Yin, L. C.; Zhang, Z. H.; Cheng, J. J. *Biomacromolecules* **2013**, *14*, 3706−3712.
(42) Xing, H.; Tang, L.; Yang, X.; Hwang, K.; Wang, W.; Yin, Q.; Wong, N. Y.; Dobrucki, L. W.; Yasui, N.; Katzenellenbogen, J. A.; Helferich, W. G.; Cheng, J.; Lu, Y. *J. Mater. Chem. B* **2013**, *1*, 5288−5297.
(43) Graf, N.; Bielenberg, D. R.; Kolishetti, N.; Muus, C.; Banyard, J.; Farokhzad, O. C.; Lippard, S. J. *ACS Nano* **2012**, *6*, 4530−4539.
(44) Dhar, S.; Gu, F. X.; Langer, R.; Farokhzad, O. C.; Lippard, S. J. *Proc. Natl. Acad. Sci. U.S.A.* **2008**, *105*, 17356−17361.
(45) Huang, Y.; Tang, Z. H.; Zhang, X. F.; Yu, H. Y.; Sun, H.; Pang, X.; Chen, X. S. *Biomacromolecules* **2013**, *14*, 2023−2032.
(46) Scarano, W.; Duong, H. T.; Lu, H.; De Souza, P. L.; Stenzel, M. H. *Biomacromolecules* **2013**, *14*, 962−975.
(47) Zhu, W.; Li, Y. L.; Liu, L. X.; Chen, Y. M.; Wang, C.; Xi, F. *Biomacromolecules* **2010**, *11*, 3086−3092.
(48) Aryal, S.; Hu, C. M. J.; Zhang, L. F. *ACS Nano* **2010**, *4*, 251−258.
(49) Duong, H. T. T.; Huynh, V. T.; de Souza, P.; Stenzel, M. H. *Biomacromolecules* **2010**, *11*, 2290−2299.
(50) Kolishetti, N.; Dhar, S.; Valencia, P. M.; Lin, L. Q.; Karnik, R.; Lippard, S. J.; Langer, R.; Farokhzad, O. C. *Proc. Natl. Acad. Sci. U.S.A.* **2010**, *107*, 17939−17944.
(51) Yang, J.; Liu, W.; Sui, M.; Tang, J.; Shen, Y. *Biomaterials* **2011**, *32*, 9136−9143.
(52) Peng, J. R.; Qi, T. T.; Liao, J. F.; Chu, B. Y.; Yang, Q.; Li, W. T.; Qu, Y.; Luo, F.; Qian, Z. Y. *Biomaterials* **2013**, *34*, 8726−8740.
(53) Song, H. Q.; Wang, R.; Xiao, H. H.; Cai, H. D.; Zhang, W. J.; Xie, Z. G.; Huang, Y. B.; Jing, X. B.; Liu, T. J. *Eur. J. Pharm. Biopharm.* **2013**, *83*, 63−75.
(54) Chen, C.; Chen, L.; Cao, L. P.; Shen, W. J.; Yu, L.; Ding, J. D. *RSC Adv.* **2014**, *4*, 8789−8798.
(55) Yu, L.; Xu, W.; Shen, W. J.; Cao, L. P.; Liu, Y.; Li, Z. S.; Ding, J. D. *Acta Biomater.* **2014**, *10*, 1251−1258.
(56) Yu, L.; Zhang, Z.; Zhang, H.; Ding, J. D. *Biomacromolecules* **2009**, *10*, 1547−1553.
(57) Siepmann, J.; Peppas, N. A. *Adv. Drug Delivery Rev.* **2001**, *48*, 139−157.
(58) Peng, K. T.; Chen, C. F.; Chu, I. M.; Li, Y. M.; Hsu, W. H.; Hsu, R. W. W.; Chang, P. J. *Biomaterials* **2010**, *31*, 5227−5236.
(59) Lynd, N. A.; Meuler, A. J.; Hillmyer, M. A. *Prog. Polym. Sci.* **2008**, *33*, 875−893.
(60) Kwon, K. W.; Park, M. J.; Bae, Y. H.; Kim, H. D.; Char, K. *Polymer* **2002**, *43*, 3353−3358.
(61) Jeong, B.; Bae, Y. H.; Kim, S. W. *Colloids Surf., B* **1999**, *16*, 185−193.
(62) Xue, X.; Hall, M. D.; Zhang, Q.; Wang, P. C.; Gottesman, M. M.; Liang, X. J. *ACS Nano* **2013**, *7*, 10452−10464.